

# **Fabrication and Characterization of PVDF - PZT (Navy type-VI) composites**

A Thesis Submitted in Partial Fulfilment of the  
Requirements for the Degree of

## **Bachelor of Technology**

By

**Swetapadma Mahapatra (Roll No.110cr0453)**

Supervisor:

**Prof. Ranabrata Mazumder**



**Department of Ceramic Engineering,  
National Institute of Technology, Rourkela,  
Odisha.**

## *ACKNOWLEDGEMENT*

With deep regards and profound respect, I avail this opportunity to express my deep sense of gratitude and indebtedness to Prof. Ranabrata Mazumder, Department of Ceramic Engineering, N.I.T. Rourkela, for introducing the present research topic and for inspiring guidance, constructive criticism and valuable suggestion throughout this research work. It would have not been possible for me to bring out this project report without his help and constant encouragement. I wish that he will keep in touch with me in future and will continue to give his valuable advice.

I would like to express my gratitude to all the faculties of Department of Ceramic Engineering as well as technical and non-technical employee of the department whose vast knowledge in the field of science and technology has enlightened me in different areas of this experimental research work. I am also thankful to Mr. Ganesh Sir, Mr, Jayrao Sir and Mrs. Pratibha Madam for helping me in the lab.

Above all, I thank GOD for giving me the encouragement, skills and opportunity to complete this report.

(SWETAPADMA MAHAPATRA)



## National Institute of Technology Rourkela

### CERTIFICATE

This is to certify that the thesis entitled, “*Fabrication and Characterization of PVDF - PZT (Navy type-VI) composites*” submitted by Ms. **Swetapadma Mahapatra** in partial fulfilments for the requirements for the award of **Bachelor of Technology** degree in **Ceramic Engineering** at National Institute of Technology, Rourkela is an authentic work carried out by her under my supervision and guidance.

To the best of my knowledge, the matter embodied in the thesis has not been submitted to any other University/ Institute for the award of any Degree or Diploma.

Date: 12-05-2014

Prof Ranabrata Mazumder  
Dept. of Ceramic Engineering  
National Institute of Technology  
Rourkela-769008

## CONTENTS

Sl No.	Title	Page No.
	<i>Acknowledgement</i>	2
	<i>Abstract</i>	5
	<i>List of Tables</i>	6
	<i>List of Figures</i>	6
1	Introduction	7-8
2	Literature Survey	9-19
2.1	Ferro electricity	10
2.2	Lead Zirconate Titanate (PZT)	12
2.3	Polyvinylidene Flouride (PVDF)	16
2.4	Ceramic Polymer Composite	17
3	Experimental Procedure	20-24
4	Results and Discussion	25-34
4.1	Density Measurements	26
4.2	Phase identification by XRD	29
4.3	Dielectric Properties of the composites	31
4.4	Microstructure of the films	33
5	Conclusion and Scope for future work	35-36
6	References	37

## **ABSTRACT**

Our work comprises preparation of homogeneous ceramics-polymer composites consisting of PZT (Navy Type VI) particles in the form of fillers and PVDF polymer as matrix, using a solution casting process. The structural, microstructural and dielectric properties of the composites film were investigated by X-ray Diffraction, Field Emmission Scanning Electron Microscopy, LCR Meter, respectively and discussed. The X-ray diffraction patterns indicate that with the addition of PZT, the polymer peak gradually flattens. PVDF matrix of the PVDF-PZT composite is contains mixture of  $\alpha$  and  $\beta$  phase. The FESEM images show a uniform distribution of ceramic fillers in the polymer matrix. The composites prepared show greater dielectric permittivity and a reduced loss tangent. The results suggest that the introduced ceramic PZT fillers have a good influence on the polymer matrix and contribute to the improvement of the dielectric behaviour of the composites.

## List of Figures

Sl No.	Title	Page No.
1	Idealized permittivity of a ferroelectric material as a function of temperature	11
2	Phase stabilities in the $\text{PbZrO}_3\text{-PbTiO}_3$ system	13
3	Coupling coefficient $k_p$ and permittivity $\epsilon$ values across the PZT compositional range	13
4	Schematic of orientation of fluoride ions in $\alpha$ , $\beta$ phase of PVDF	16
5	Diagram for formation of different PVDF phase	17
6	Connectivity families for diphasic composites	18
7(a)	Measured and calculated bulk density of composites at different volume fractions of PZT	27
7(b)	Relative density and calculated porosity of composites at different volume fractions of PZT.	27
8(a)	XRD patterns of PVDF film	29
8(b)	XRD patterns of composite with 10 vol.% of PZT	29
8(c)	XRD patterns of composite with 50 vol.% of PZT	29
9(a)	Frequency dependence of relative permittivity ( $\epsilon_r$ ) (measured at room temperature) of PVDF- PZT(Navy type VI) composite as functions of frequency for different volume percent of PZT-0, 10, 20 vol% PZT	31
9(b)	Frequency dependence of relative permittivity ( $\epsilon_r$ ) (measured at room temperature) of PVDF- PZT (Navy type VI) composite as functions of frequency for different volume percent of PZT - 0-50 vol% PZT	31
10	Frequency dependence of dielectric loss ( $\tan \delta$ ) (measured at room temperature) of PVDF-PZT (Navy type VI) composite as functions of frequency for different volume percent of PZT.	32
11(a)	FESEM images of PVDF film (0% filler)	33
11(b)	FESEM images of PVDF film (10% filler)	33
11(c)	FESEM images of PVDF film (50% filler)	34

## List of tables

Sl No.	Title	Page No.
1	Common aliovalent substitutions of PZT ceramics and their effects on properties	15
2	Amount of PZT to be added	22
3	Density data calculations	26

**CHAPTER 1**  
**INTRODUCTION**

Global energy consumption has gradually increased in the past decades due to industrialization and population growth. Our society is facing a problem with the depletion of fossil energy resources as well as environmental problems (such as global warming, carbon dioxide emissions, and damage to the ozone layer). Renewable energy sources can be seen as the only possible solution to tackle this problem. One way of to harvest energy is to utilize piezoelectric materials that can convert mechanical and vibrational energy into electrical energy [1]. Another requirement is high energy storage materials which can increase the efficiency of electric power system. Large dielectric permittivity and high electrical breakdown strength are two essential factors to attain high energy density. Low dielectric loss, fast charge and discharge speed, and cheap cost are also important factors for energy storage applications [2].

For first need we require flexible efficient ferroelectric/piezoelectric materials and for second case high dielectric constant, low loss and high breakdown strength materials are the requirement. Ceramic ferroelectric/piezoelectric materials are unsuitable for both these application. Polymer ferroelectric also have inferior dielectric and piezoelectric properties restrict their application. Ferroelectric ceramic-polymer composite could be a great option for those applications. . Hence a solution can be to fabricate ceramics-polymer composites comprising of ceramic fillers of large dielectric permittivity and the polymer matrix of high electrical breakdown strength. Some works have been done to investigate the ceramics polymer composites. As the dielectric properties and electrical breakdown strength are strongly influenced by the homogeneity of the composites, it is important to improve the agglomeration of the ceramic fillers in the polymer matrix. Furthermore, the influence of the incorporation of the ceramic fillers also requires thorough investigation. Composite piezoelectric also have found its application in transducer, ultrasonic medical imaging and non-destructive evaluation. They have also found application as actuators and in micro-motors.

Ceramic-polymer piezoelectric composites are being studied in the desire to obtain the optimum electromechanical and physical properties. Ferroelectric composites are classified according to their connectivity. For a diphasic composite, there exist 16 connectivity patterns. Of these, 0–3 and 1–3 composites are most studied because of their outstanding properties and relative ease of fabrication [3]. Ceramics [BaTiO<sub>3</sub>, PZT (Lead Zirconate Titanate), CCTO (Calcium Copper Titanate)] are generally studied because of their high dielectric permittivity but they have low energy storage capacity as they have a low breakdown strength. On the other hand polymers such as [poly (vinylidene fluoride) (PVDF), Polypropylene (PP), Polyethylene (PE)] have high electrical breakdown strength but these polymer materials always exhibit low dielectric permittivity or high dielectric loss [2].



**CHAPTER 2**  
**LITERATURE**  
**SURVEY**

## 2.1 Ferroelectricity

When an electric field is applied to an ideal *dielectric* material there is no long-range transport of charge but only a limited rearrangement of charge such that the dielectric acquires a dipole moment and is said to be polarized. Atomic polarization, which occurs in all materials, is a small displacement of the electrons in an atom relative to the nucleus. In ionic materials there is, in addition, ionic polarization involving the relative displacement of cation and anion sublattices. Dipolar materials, such as water, can become polarized because the applied electric field orients the molecules. Finally, space charge polarization involves a limited transport of charge carriers until they are stopped at a potential barrier, possibly a grain boundary or phase boundary.

An individual atom or ion in a dielectric is not subjected directly to an applied field but to a local field which has a very different value and under certain conditions, lattice polarization produces a local field which tends to stabilize the polarization further – a feedback mechanism. This points to the possibility of “*spontaneous polarization*” i.e., lattice polarization in the absence of an applied field. Such spontaneously polarized materials do exist and “ferroelectrics” constitute an important class among them. The two conditions necessary in a material to classify it as a *ferroelectric* are (1) the existence of spontaneous polarization and (2) a demonstrated reorientation of the polarization by an applied electric field [4].

Generally, ferroelectric materials possess high dielectric constant and they are piezoelectric.

At a particular temperature, nearly all ferroelectric materials pass through a ferroelectric to paraelectric phase transition (in several examples materials decompose prior to passing into the paraelectric state) [4]. The temperature at which a ferroelectric material reverts to the high temperature paraelectric phase is called the Curie temperature ( $T_C$ ). On cooling through  $T_C$  into a ferroelectric phase, a reorientable spontaneous polarization is developed.

In ferroelectrics dominated by a displacive phase transition, such as perovskite materials, the temperature dependence of the permittivity varies for 1st and 2nd order phase transitions. Fig. 1 illustrates the temperature dependence of the permittivity for displacive ferroelectric materials exhibiting first or second order phase transitions. Second order phase transitions, which are common for rhombohedral compositions, are generally characterized by a broad peak in permittivity. Ferroelectrics undergoing first order phase transitions, typical of tetragonal perovskite materials, however show a fairly flat permittivity with increasing temperature right up to the  $T_C$ .

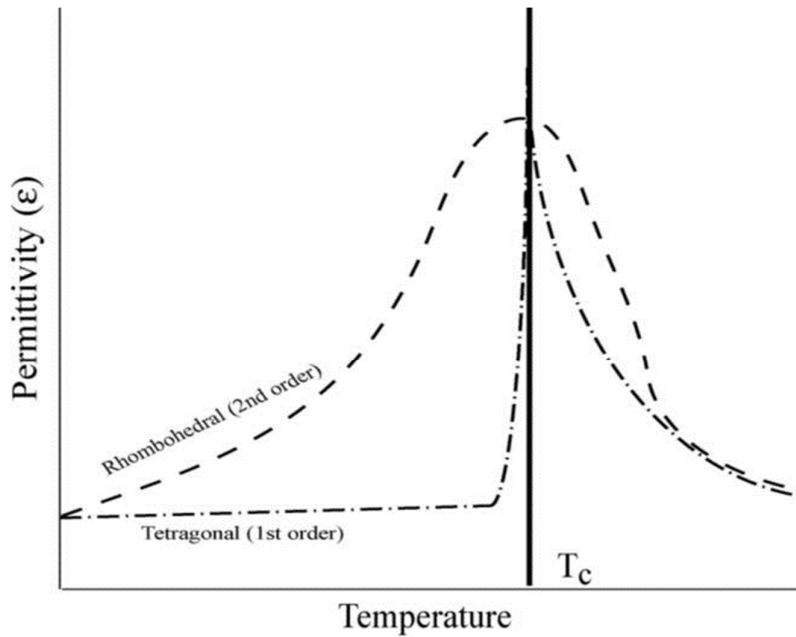


Fig.1 Idealized permittivity of a ferroelectric material as a function of temperature.

The reciprocal permittivity  $1/\epsilon$  is known to be linear with respect to the temperature in a wide range in the paraelectric phase (so-called Curie-Weiss law),

$$\epsilon = \frac{C}{T - T_0}$$

where  $C$  is the Curie-Weiss constant and  $T_0$  the Curie-Weiss temperature.  $T_0$  is slightly lower than the exact transition temperature  $T_c$ . For displacive transitions (e.g.,  $\text{BaTiO}_3$ ,  $\text{PbTiO}_3$ ,  $\text{KNbO}_3$ ), the Curie Constant is very high ( $\sim 10^4 - 10^5$  K) and the paraelectric phase is microscopically nonpolar. For order-disorder transition (e.g., TGS,  $\text{KH}_2\text{PO}_4$ ), the Curie Constant is of the order of  $T_0$  and the paraelectric phase is nonpolar on macroscopic or thermally averaged sense.

Normally, ceramic ferroelectrics may be classified into four groups depending on their crystal structure: (1) the oxygen octahedral group (perovskite) (2) the tungsten-bronze group, (3) the pyrochlore group and (4) the bismuth layer-structure group. Of these, the  $\text{ABO}_3$  perovskite type is by far the most important category, economically. The families of compositions, e.g.,  $\text{BaTiO}_3$ , PZT (lead zirconate titanate), PLZT (lead lanthanum zirconate titanate), PT (lead titanate), PMN (lead magnesium niobate), and  $(\text{Na,K})\text{NbO}_3$  represent the bulk of the ferroelectric ceramics manufactured in the world today.

Most technologically important ferroelectrics are oxides with a perovskite structure. The great sensitivity of ferroelectrics to chemistry, defects, electrical boundary conditions and pressure arises from a delicate balance between the long range coulomb force (which favours the ferroelectric state) and short range repulsion (which favours the non-polar cubic structure) [5,6].

## 2.2 Lead zirconate titanate (PZT)

PZT is a solid solution of  $\text{PbZrO}_3$  and  $\text{PbTiO}_3$  and the compositions around  $\text{Pb}(\text{Zr}_{0.52}\text{Ti}_{0.48})\text{O}_3$  are of technical importance. PZT and modified PZT are materials of choice for transducer applications because they (1) possess higher electromechanical coupling coefficients than  $\text{BaTiO}_3$ , (2) have higher  $T_C$  values, which permit higher temperature of operation or higher temperature of processing during fabrication of the devices, (3) can be easily poled, (4) possess a wide range of dielectric constants, (5) are relatively easy to sinter at lower temperatures than  $\text{BaTiO}_3$ , and (6) form solid-solution compositions with many different constituents, thus allowing a wide range of achievable properties.

The PZT phase diagram is shown in Fig.2 where it can be seen that the morphotropic phase boundary (MPB) is a significant feature. An MPB denotes an abrupt structural change with composition at constant temperature in a solid solution range. In the PZT system it occurs close to the composition where  $\text{PbZrO}_3$ :  $\text{PbTiO}_3$  is 1:1 (molar). At composition near the MPB the coupling coefficient and the relative permittivity peak as shown in Fig.3 and this feature is exploited in commercial compositions.

Our goal is to fabricate PVDF - PZT(Navy type-VI) composite film by simple solution casting method, to study the phase evolution, density, microstructure and dielectric properties of composites with PZT(Navy type-VI) volume fraction in the range of 0–50 vol.% (0,10,20,30,40,50).

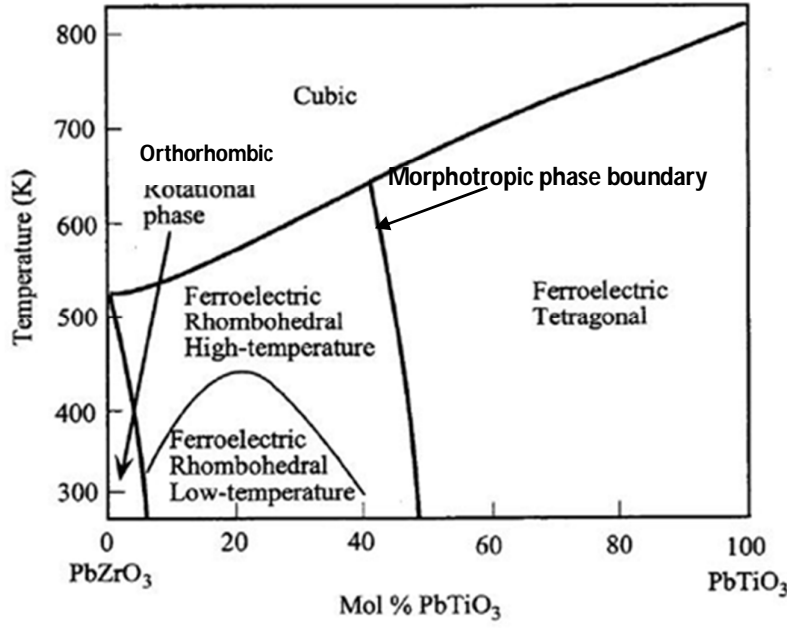


Fig.2 Phase stabilities in the  $\text{PbZrO}_3$ - $\text{PbTiO}_3$  system

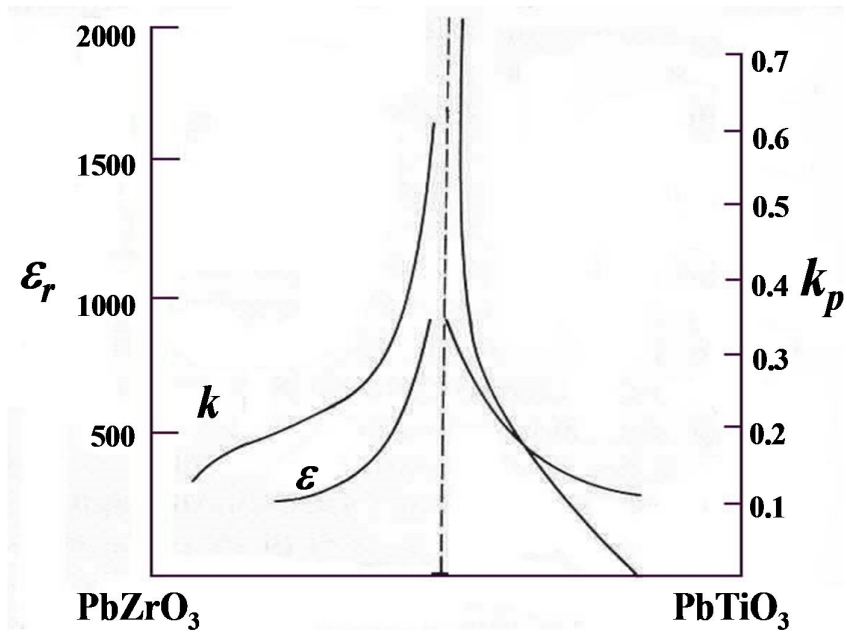


Fig. 3 Coupling coefficient  $k_p$  and permittivity  $\epsilon$  values across the PZT compositional range.

The changes in directions of the spontaneous polarization require small ionic movements in specific crystallographic directions. It follows that the greater is the number of possible directions the more closely the polar axes of the crystallite in a ceramic can be brought to the direction of the poling field. The tetragonal ( $4mm$ ) structure allows six directions, while the rhombohedral ( $3m$ ) allows eight and so should permit greater alignment. If both tetragonal and rhombohedral crystallites are present at a transition point, where they can be transformed from one to the other by a field, the number of alternative crystallographic directions rises to 14 and the extra alignment attained becomes of practical significance [4].

A number of compositional modifications have been studied in the PZT system. The purposes of these modifications were to improve sintering, to control microstructure, and ultimately, to substantially improve the properties for various types of applications.

Undoped PZT ceramics usually have p-type conductivity, which can be attributed to an excess of Pb vacancies over oxygen vacancies because of the loss of volatile PbO during firing. Electrons are then trapped at Pb vacancies, leaving holes in the lattice. Donor doping thus reduces the hole conductivity, leading to an increase in the resistivity of the ceramics, typically by orders of magnitude. The underlying mechanism can be understood by the mass action law, which requires that the product of electron and hole concentrations remains constant [5].

The types of modifications to PZT ceramics, which have been studied by replacement of some of the cations in the structure, include: isovalent, compensating valent, and aliovalent substitutions. Substitution of  $Pb^{2+}$  by  $Sr^{2+}$ , or  $Ca^{2+}$  and  $Ba^{2+}$  are typical isovalent substitutions. The general effects are a lowering of the Curie temperature, an increase in the longitudinal piezoelectric coefficient ( $d_{33}$ ), and a slight increase in the electromechanical coupling efficiency. A solid solution between PZT and PMN is an example of a compensating valence substitution, in which the stoichiometry is preserved. Usually piezoelectric properties can be tailored between PZT and other end members in a complex crystalline solution series [6].

Aliovalent substitutions can be divided into two types. One is the substitution of cations by ions that are more positive in valence (such as  $Bi^{3+}$  or  $La^{3+}$ ) onto the  $Pb^{2+}$  sites or by  $Nb^{5+}$  or  $W^{6+}$  modifications onto the  $Zr^{4+}$  and  $Ti^{4+}$  sites. Such types of substitutions create

vacancies on perovskite A-sites and cause the material to be a “soft” ferroelectric. On the other hand, impurities of a lower valence (e.g.  $\text{Fe}^{3+}$ ,  $\text{Mg}^{2+}$ ,  $\text{K}^{1+}$ ) than the host cations generate vacancies on oxygen sites. These substitutions result in “hard” ferroelectrics, which have the opposite effects to those of higher valence substitutions. Table 1 summarizes common aliovalent substitutions for PZT ceramics and their effects on the properties. Soft ferroelectrics have lower coercive fields, higher hysteretic losses, higher dielectric and mechanical loss factors, and lower remanent polarizations and strains relative to hard ones. Most of these effects can be explained as a result of vacancies facilitating domain boundary motion. Hard ferroelectrics have an asymmetric P–E response, which is shifted by a built-in potential. The built-in potential generates from the pinning of the polarization by dipolar defects [7].

**Table 1** Common aliovalent substitutions of PZT ceramics and their effects on properties [8]

Additives causing A-site vacancies	Additives causing O-site vacancies
$(\text{Pb}^{2+}: \text{Bi}^{3+}, \text{La}^{3+}, \text{Zr}^{4+})$ or $(\text{Ti}^{4+}: \text{Nb}^{5+}, \text{Ta}^{5+}, \text{Sb}^{5+}, \text{W}^{6+})$	$(\text{Pb}^{2+}: \text{K}^{1+}, \text{Zr}^{4+})$ or $(\text{Ti}^{4+}: \text{Mg}^{2+}, \text{Sc}^{3+}, \text{Fe}^{3+})$
Increased dielectric constant	Relatively low dielectric Constant
High dielectric loss	Low dielectric loss
Increased elastic compliance	Moderately lowered electrical resistivity
Low mechanical Q	High mechanical Q
High piezoelectric coupling factor	High coercive field
Low coercive field	More difficult poling and depoling
Relatively square hysteresis loop	Relatively dark color
Greatly increased electric volume resistivity	Relative insensitivity to darkening by light
Anomalously small aging Effects	
Easy nonelastic mechanical deformation	
Yellow color	
Translucency	
Easy phototropic darkening	

Different type of commercial grade PZT is available in market; they are PZT-2, PZT-4, PZT-5A, PZT-5H, and PZT-8. PZT-(Navy type VI) or PZT 5-H has even higher sensitivity and permittivity ( $\epsilon_r = 3500$ ) than most other compositions. It has lower Curie temperature ( $190^\circ\text{C}$ ).

### 2.3 PVDF (polyvinylidene fluoride)

Poly(vinylidene fluoride) (PVDF) is one of the semicrystalline polymers with at least four crystalline phases, famous for its pyroelectric, piezoelectric and ferroelectric properties [9]. PVDF can form a different crystal depending on the condition of the crystallization. The different crystal structures are nonpolar  $\alpha$ -phase, polar  $\beta$  - ,  $\gamma$  - phase and  $\delta$ -phase [10]. When PVDF is cooled from the melt, the crystalline phase formed is the nonpolar  $\alpha$ -phase with TGTG conformation (shown in fig. 4). The  $\beta$  -phase crystal has all trans conformation that results in the most polar phase among other crystals, being used extensively in piezoelectric, pyroelectric and ferroelectric applications. The b-phase is typically obtained by mechanical deformation of melt-crystallized films (shown in fig. 5).

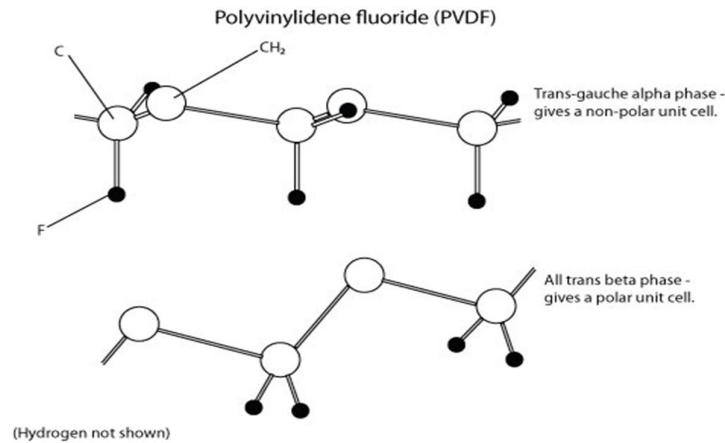


Fig. 4 Schematic of orientation of fluoride ions in  $\alpha$ ,  $\beta$  phase of PVDF



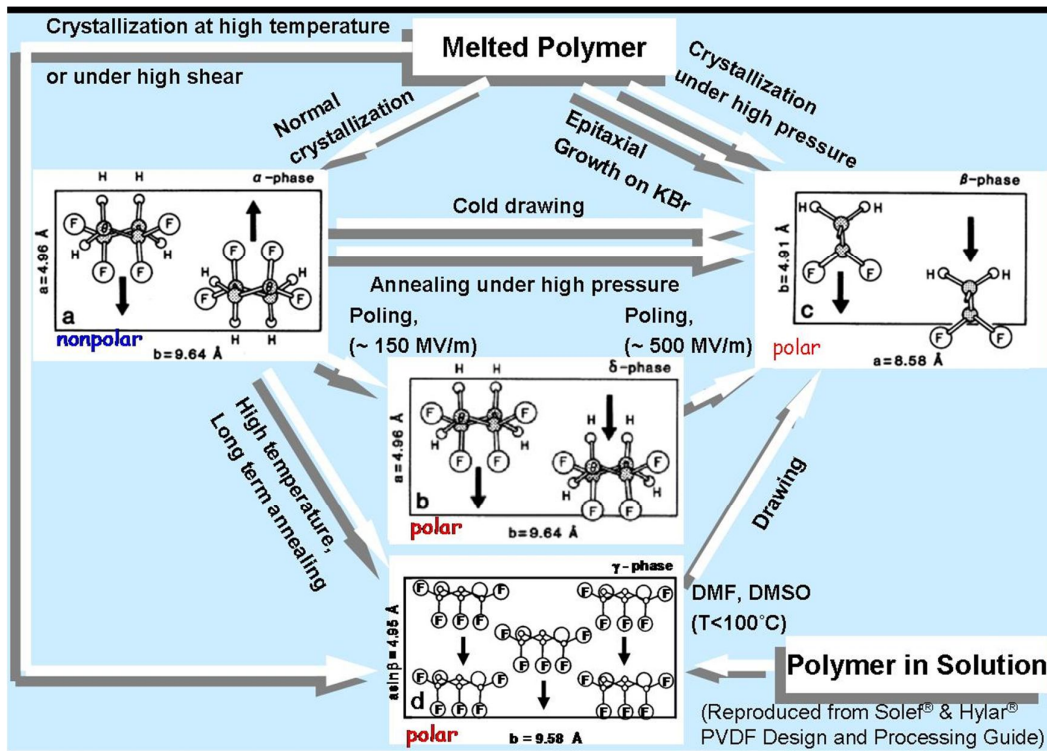


Fig. 5 Diagram for formation of different PVDF phase [10]

## 2.4 Ceramic Polymer Composite:

Ceramic polymer composites comprises of a ceramic phase in a polymer phase. Their properties depend on connectivity, volume percentage of ceramic phase and distribution of the active ceramic phase in the composite. The connectivity model was developed by Newnham, Skinner and Cross (shown in Fig. 6). Connectivity refers to the arrangement of the component phases in the composite. For eg. A-B

where, A=number of ways in which the one phase is self-connected

B= number of ways in which the another phase is self-connected

Diphasic composites are of 10 types:

0-0, 1-0, 2-0, 3-0, 1-1, 2-1, 3-1, 2-2, 3-2, 3-3

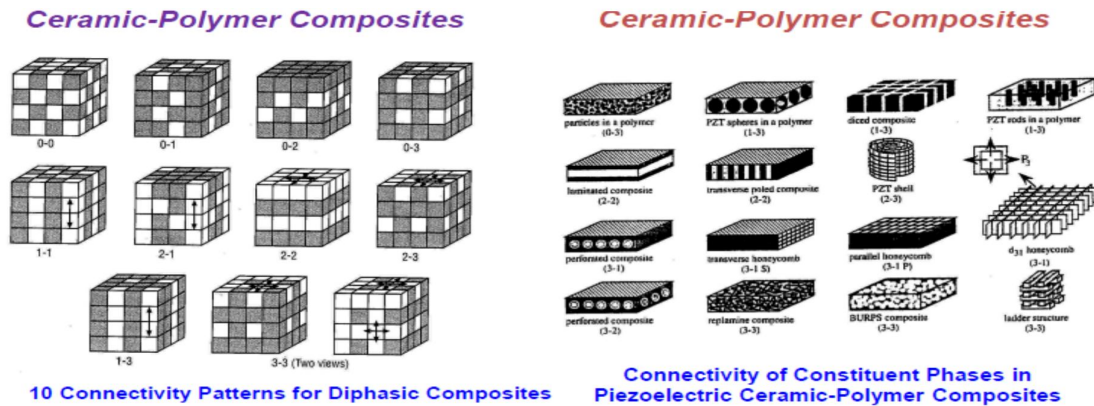


Fig. 6 Connectivity families for diphasic composites [3]

Of the above mentioned 10 types, the 3–3, 1–3, 0–3 connectivity composites are the most extensively studied while the other types are investigated less extensively due to the difficulty in fabrication process. The 3–3 composites have ceramic and polymer in three-dimensional connectivity: they have highly sensitive hydrostatic pressure, low permittivity, and low density; however, they are not flexible. The 1–3 composites have a ceramic phase with one-dimensional connectivity in a polymer matrix: they have superior piezoelectric properties but a high fabrication cost; and the electrical properties fluctuate significantly in relation to the position of the electrodes. The 0–3 composites consist of piezoelectric ceramic powders dispersed in a polymer matrix: they have a low figure of merit but are simple to fabricate; and the shape of the product can be varied easily, which facilitates mass production; in addition, their good flexibility means that the fabrication process can also be varied, which is why this type of composite has been the most actively researched.

Seema et. al.[11] reported preparation of PVDF-PZT(5-H) composites by an unconventional route, which combines the solution and melt processing technique to ensure uniform distribution of filler. A comparative study of hot press and tape casting technique were done with respect to physical and dielectric characteristics of the composites with varying ceramic contents (20–60 vol %). They found that Density of the composites was 2.74 to 5.13 g/cm<sup>3</sup> as PZT concentration increased from 20 to 60 volume fractions. The dielectric constant of composites at 1 MHz varied from 16.74 to 98.48 as PZT concentration increased from 20 to 60 volume fractions.

Anjana et. al.[12] reported fabrication of PVDF-PZT films by using a solvent cast method. They shows that prepared films are in  $\beta$  -phase, which are in all trans TTTT

conformation. Surface features show that PZT is uniformly distributed in PVDF, and infrared spectrum further confirms the presence of  $\beta$ -phase. The DSC scans indicate that the degree of crystallinity increases with PZT weight fraction, and the tensile modulus and strength with 50% weight fraction of PZT are found to be 1574 and 8.5 MPa, respectively.

Zak et.al.[13] reported fabrication of Poly(vinylidene fluoride)/lead zirconate titanate nanocomposite thin films (PVDF/PZT-NPs) by mixing fine  $\text{Pb}(\text{Zr}_{0.52},\text{Ti}_{0.48})\text{O}_3$  nanoparticles (PZT-NPs) into a PVDF solution under ultrasonication. The mixture was spin coated onto glass substrate and then cured at  $110^\circ\text{C}$ . The dielectric properties of the PVDF/PZT-NPs were analyzed in detail with respect to frequency. In comparison with pure poly (vinylidene fluoride), the dielectric constant of the nanocomposite (15 vol.% PZTNPs) was increased, whereas the loss tangent was unchanged in the frequency range of 100 Hz to 30 MHz. The nanocomposites exhibited good dielectric stability over a wide frequency range.

### **Objective**

Our goal is to fabricate PVDF - PZT(Navy type-VI) composite film by simple solution casting method, to study the phase evolution, density, microstructure and dielectric properties of composites with PZT(Navy type-VI) volume fraction in the range of 0–50 vol.% (0, 10, 20, 30, 40, 50).

**CHAPTER 3**  
**EXPERIMENTAL**  
**PROCEDURE**

Our aim is to prepare films of pure PVDF and PVDF-varying concentration of PVDF composites through solvent casting method. We have decided to go for the preparation of films of the following compositions:

- Pure PVDF
- PVDF+10 vol% PZT
- PVDF+20 vol% PZT
- PVDF+30 vol% PZT
- PVDF+40 vol% PZT
- PVDF+50 vol% PZT

For our project work Sparkler 5-H was used as PZT source. Surface area of the PZT powder was  $1.595 \text{ m}^2/\text{gm}$ . Particle size of the was  $0.5 \text{ }\mu\text{m}$ . PVDF powder was used from Alfa Aesar.

Our first step is to properly mix the PVDF powder in the solvent (in our case, we have used DMF (N-N Dimethyl formamide)). The mixture was stirred with the help of a magnetic stirrer for 1 hour. After experimenting with a wide range of PVDF content in a fixed amount of DMF solvent it was noted that the maximum workable range of viscosity is till the addition of 1.25g of PVDF in 12.5 ml of DMF solvent. For all the film preparation this amount of PVDF in the solvent was kept constant. Now for the composite film preparation only the amount of PZT was varied in terms of vol% of the amount of PVDF taken.

For example, to prepare a 10 vol% PZT-PVDF mixture the amount of PZT to be mixed is calculated as:

$$\text{PVDF}=1.25\text{g}$$

$$\text{Density (PVDF)} =1.78\text{g/cc}$$

$$\text{Volume}=\text{M/D}=1.25/1.78=0.702\text{cc}$$

$$\text{PZT}=10 \text{ vol\% of PVDF}=0.1*0.702=0.0702\text{cc}$$

$$\text{Density (PZT)} =7.5\text{g/cc}$$

$$\text{Mass}=\text{Vol}*D =0.0702*7.5 =0.526\text{g}$$

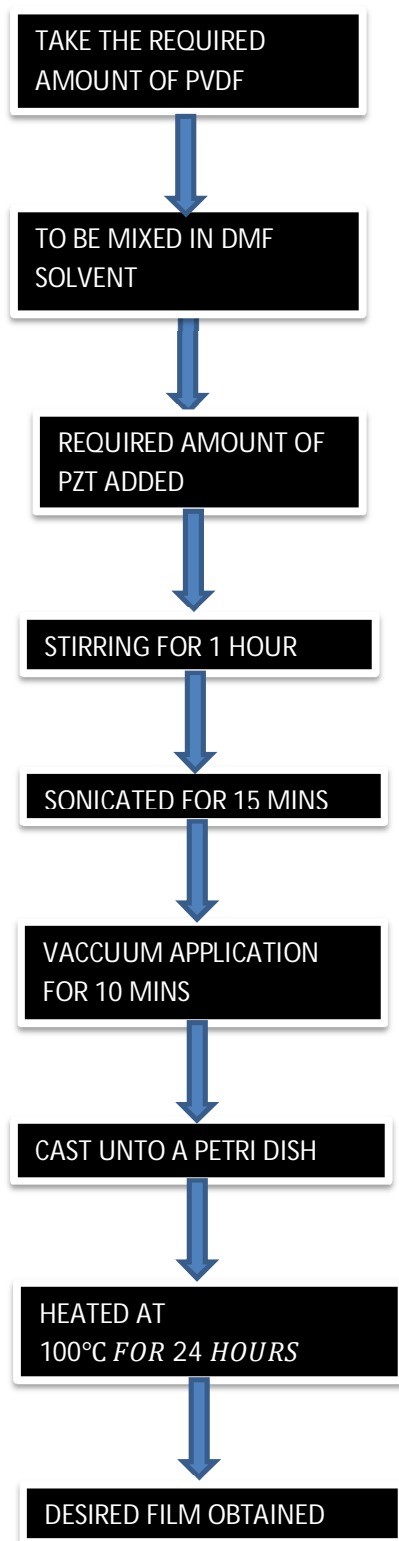
The other compositions can be calculated in a similar fashion.

TABLE 2

COMPOSITION	DMF SOLVENT TAKEN(ml)	AMOUNT OF PVDF(g)	AMOUNT OF PZT(g)
PURE PVDF	12.5	1.25	0
PVDF+10 VOL% PZT	12.5	1.25	0.525
PVDF+20 VOL% PZT	12.5	1.25	1.05
PVDF+30 VOL% PZT	12.5	1.25	1.57
PVDF+40 VOL% PZT	12.5	1.25	2.1
PVDF+50 VOL% PZT	12.5	1.25	2.6

Table 2 shows the amount of PVDF, PZT and solvent taken to prepare different PVDF-PZT composite. The mixture of the PVDF and PZT (of respective amount, required for different compositions) was stirred with the help of a magnetic stirrer for 1 hour. After proper mixing, the solution was sonicated for 15 mins. Then it was placed in a desiccator for vacuum application to remove the excess bubbles from the solution. It was then subsequently cast onto a glass substrate. The solution on the substrate was then heated at 100°C for 24 hours to evaporate the residual solution. The measured thickness of the films was in the range of 0.05mm.

## Flowchart for preparation PVDF-PZT composite film



### **Characterization Techniques used on the samples:**

- Density measurements with varying PZT content
- XRD of the pure PVDF sample and the different composite films
- Measurement of dielectric permittivity with variation of frequency
- Measurement of loss factor with varying frequency
- FESEM of the pure PVDF and the composite films



**CHAPTER 4**  
**RESULTS AND DISCUSSION**

#### 4.1 Density Measurements:

The calculated values of the bulk density of composites,  $\rho_{cal}$ , are obtained using equation [14]

$$\rho_{cal} = \rho_f V_f + \rho_m (1 - V_f)$$

where,

$\rho_{cal}$  = calculated composite density,

$V_f$  = filler (ceramic) volume fraction,

$\rho_f$  = density of filler,

$\rho_m$  = matrix density.

(Density of PZT is 7.5 and density of PVDF (matrix) is 1.7 g/cm<sup>3</sup> in the calculation.)

The porosity,  $p$ , of composites can be calculated from the measured and calculated density of composites using equation

$$P = 1 - \rho_{mea} / \rho_{cal} = 1 - \rho_{rel}$$

**TABLE 3:**

VOL% PZT	Calculated Density	Measured density of the prepared film	Relative Density (in %)	Porosity (in %)
10	2.26	2.21	97.7	2.3
20	2.85	2.80	98.2	1.8
30	3.44	3.1	90	10
40	4.01	3.58	89.2	10.8
50	4.5	3.96	88	12

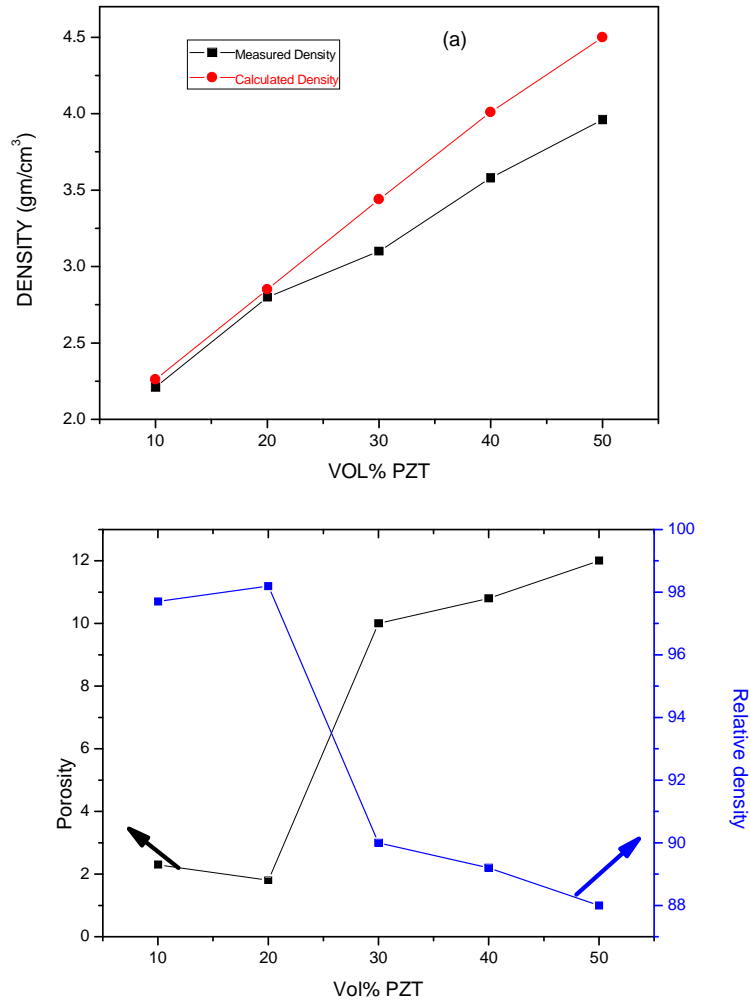


Fig.7. (a) Measured and calculated bulk density of composites at different volume fractions of PZT. (b) Relative density and calculated porosity of composites at different volume fractions of PZT.

Fig.7 shows the variation in the measured and calculated values of the bulk density of PVDF-PZT (Navy type VI) composites with the volume fraction of PZT. Obviously  $\rho_{cal}$  increases linearly with increasing  $V$  since the density of PZT ( $\rho_f = 7.5 \text{ g/cm}^3$ ) is higher than that of PVDF ( $\rho_m = 1.7 \text{ g/cm}^3$ ). However the measured bulk density exhibits a non-linear increase with increasing volume fraction of the filler and especially stays almost unchanged in the range of 40–50 vol.%. Furthermore the measured density is smaller than calculated one at fixed volume fraction of the filler, which may result from the presence of pores in composites. The deviation of the measured density from the calculated one increases with increasing volume fraction of the filler. The dependences of the relative density and the porosity of composites on the volume fraction of the filler are shown in Fig. 7(b). The relative

density (porosity) of PVDF-PZT composites decreases (increases) as the volume fraction of the PZT filler increases from 20 to 50 vol.%, indicating the increase in void formation inside the composite at higher volume fraction of the filler. It is to be noted that the flexibility of the composite could be retained when the ceramic loading was up to 50 vol.%.

## 4.2 Phase identification by XRD:

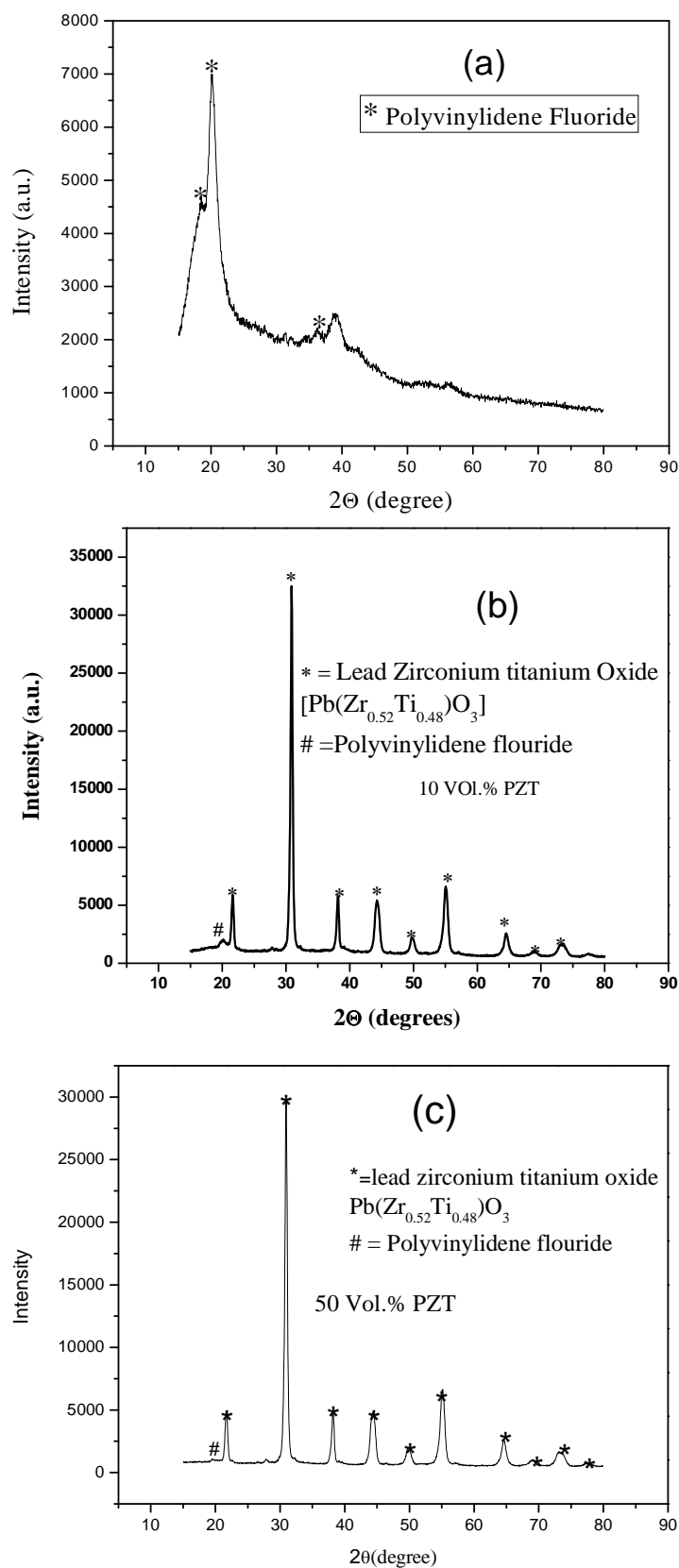


Fig.8. XRD patterns of (a) PVDF film, (b) composite with 10 vol.% of PZT, and (c) Composite with 50 vol.% of PZT.

The XRD pattern shows that the PVDF (Figure 8(a)) existed in a mixed  $\alpha$ ,  $\beta$  phase. The peak at  $2\theta$  corresponding to  $18.3(1\ 0\ 0)$  was designated to the  $\alpha$ -PVDF and  $20.05(1\ 1\ 0)$  was designated to the  $\beta$ -PVDF [15]. As can be noted in Figure 2(a) that the major peak at  $20.05$ , is the peak of  $\beta$ -PVDF. The XRD patterns that we got for the PVDF/PZT (Fig. 8b) clearly show the diffraction peaks of PZT. It can be noted that the crystal structure of PZT ceramic is tetragonal structure ( $a = 4.036 \text{ \AA}$ ,  $c = 4.014 \text{ \AA}$ ) with chemical formula  $\text{Pb}(\text{Zr}_{0.52}\text{Ti}_{0.48})\text{O}_3$ . The XRD pattern of all composites, show that no shift is observed for any of the PZT peaks in all the composite films. This confirms that the PZT structure remains the same in the composites and not affected by the presence of PVDF. The general features of the spectra in Figs 8(b) are the decreasing in peak intensities of  $\alpha$  and  $\beta$ -phases of PVDF with increasing PZT volume fractions. This is to be noted that only in 10 vol% PZT, a significant decrease in PVDF peak observed and that is due to presence of 42 wt% (equivalent to 10 vol% PZT) PZT in the composite. Fig.8(c) shows the XRD pattern of composite with 50 vol.% of PZT.

### 4.3 Dielectric Properties of the composite:

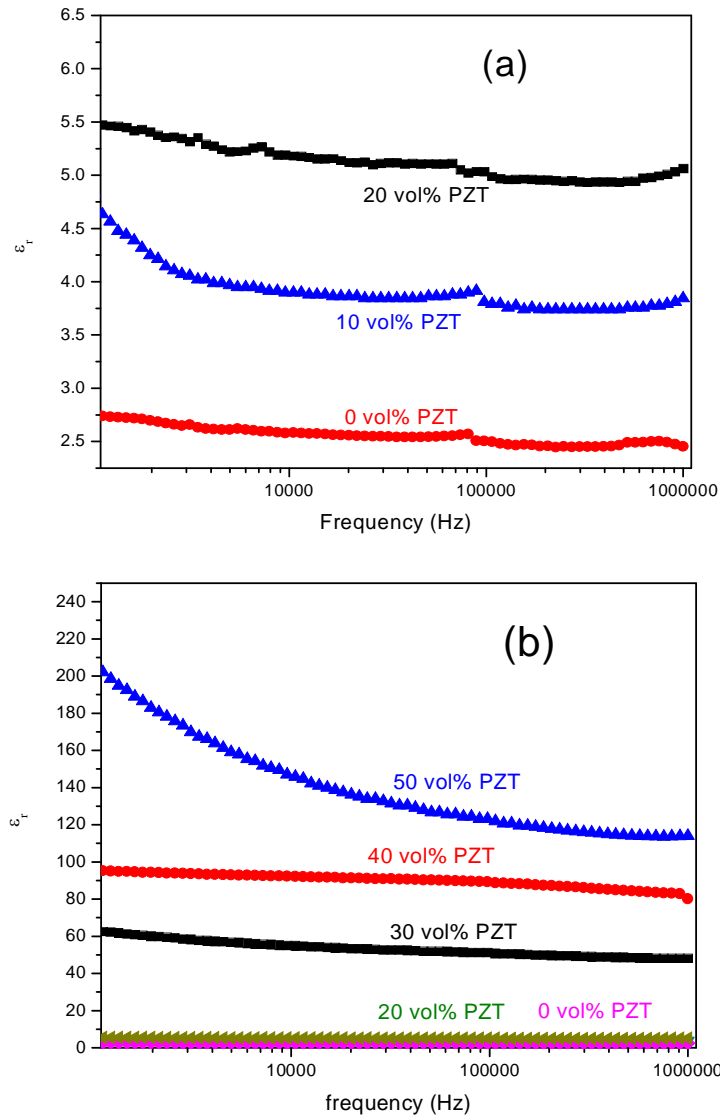


Fig. 9. Frequency dependence of relative permittivity ( $\epsilon_r$ ) (measured at room temperature) of PVDF-PZT(Navy type VI) composite as functions of frequency for different volume percent of PZT (a) 0, 10, 20 vol% PZT (b) 0-50 vol% PZT

In agreement with earlier reports, the permittivity of the composite films of varied volume fractions of PZT shows good stability in the frequency range up to  $10^6$  Hz and then decreases rapidly especially when the volume fraction of PZT is high (shown in Fig. 9). The result indicates that the decrease of the permittivity of the composite films during high frequency range is mainly due to the high frequency dielectric response of the PZT particles. However, the dielectric permittivity of the composite films increases steadily as PZT content increases over the whole frequency range as indicated in the graphs above. Especially with

the PZT (>20%) content the dielectric permittivity shows high values thus indicating a positive improvement in the matrix.

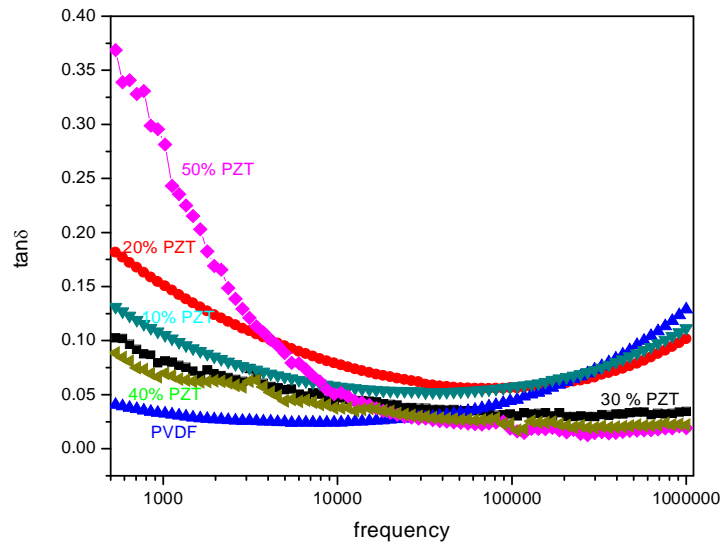


Fig.10. Frequency dependence of dielectric loss ( $\tan \delta$ ) (measured at room temperature) of PVDF-PZT(Navy type VI) composite as functions of frequency for different volume percent of PZT.

The frequency dependence of the dielectric loss of PVDF-PZT(Navy type VI) composite with different volume percent of PZT are shown in Fig.10. The loss undergoes two relaxations for pure PVDF, 10% and 20% PZT composite; one in the low frequency region and the other at high frequencies. The relaxation beyond 100 kHz is related to the glass transition relaxation of PVDF and is denoted as  $\alpha_a$  relaxation [15]. Similarly, the relaxation that appears at low frequency (<1kHz) could be attributed to  $\alpha_a$  relaxation associated with molecular motion in the crystalline regions of PVDF. In the case of composites, the loss factor is found to be decreased significantly with increase in PZT volume fraction at high frequency.



#### 4.4 Microstructure of the films:

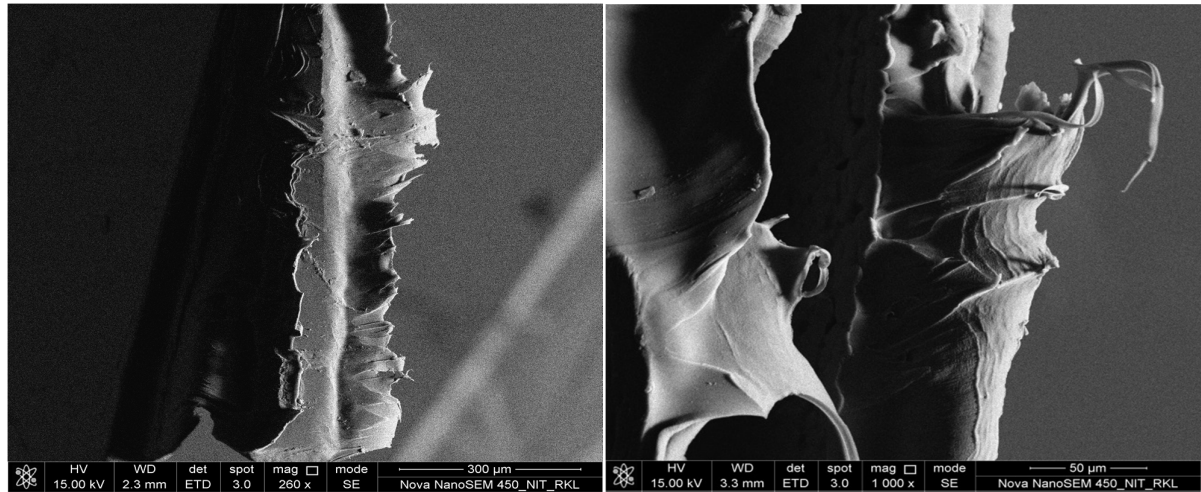


Fig.11(a) FESEM images of PVDF film (0% filler)

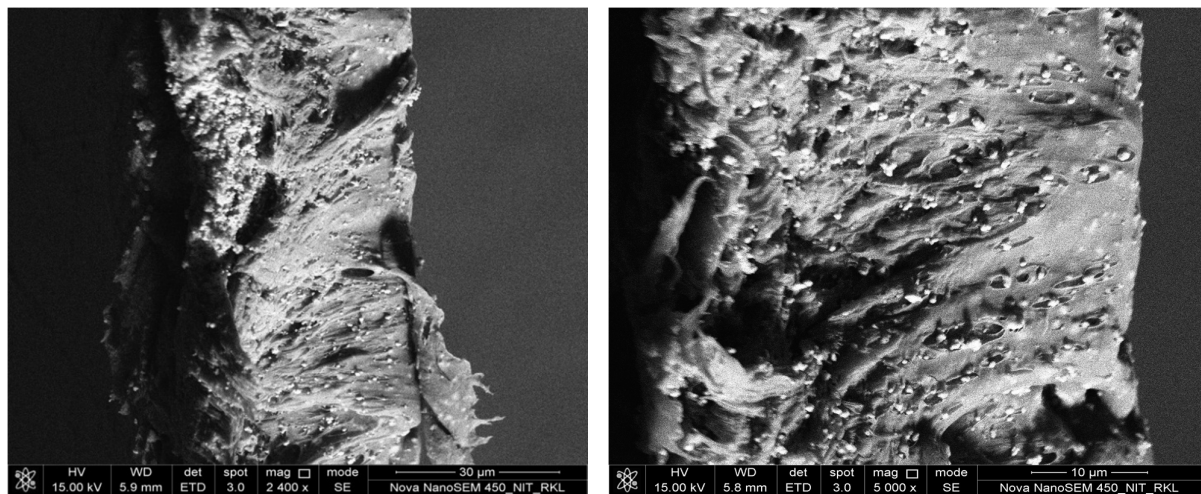


Fig.11(b) FESEM images of composite film (10 vol% PZT filler)

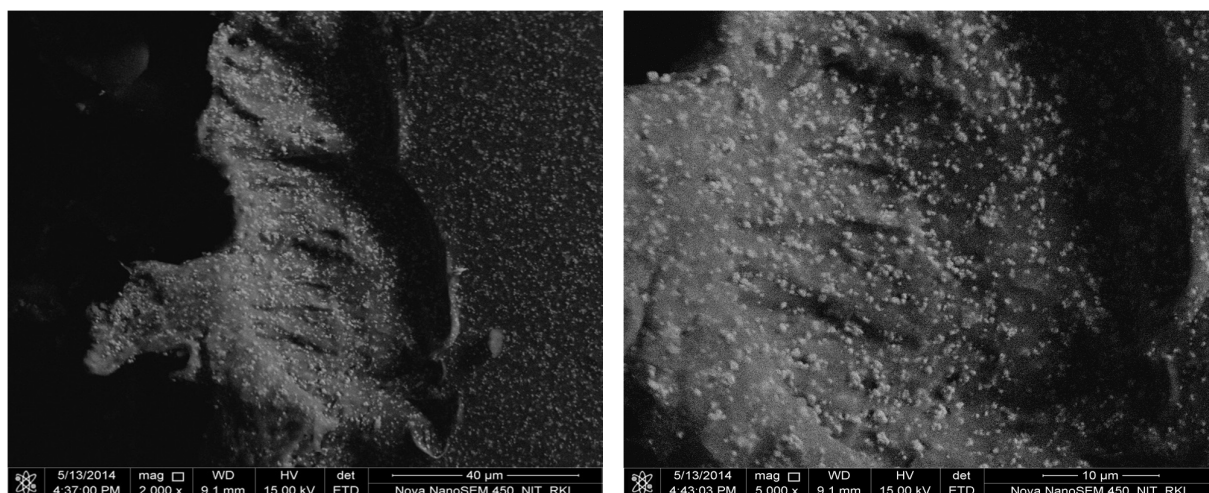


Figure 11(c) FESEM images of composite film (50 vol% PZT filler)

FESEM was carried out to get an insight into the composite microstructure and the distribution of the ceramic filler in the polymer matrix. The microstructures [Fig. 11 (a-c)] of the composites show a good distribution of the PZT fillers within the PVDF matrix. It can be seen from [Fig. 11 (b-c)] that PZT particles are of sphere like shape with an average size of  $0.5 \mu\text{m}$ . At lower volume fraction (10 vol.%), PZT particles disperse well in PVDF matrix, indicating that the ceramic filler is compatible with the matrix. At higher volume fractions (50 vol.%), most ceramic particles connect one another. In addition, pores exist in composite samples in the higher volume fraction range 30–50 vol.%. It was reported earlier [Ref.], good dispersion along with homogeneous packing of ceramic filler is likely to exhibit high dielectric constant. Indeed, we could achieve a relative permittivity as high as 180 at 1kHz for the PVDF with 50 vol.% PZT composite.

**CHAPTER 5**  
**Conclusions and Scope**  
**For Future work**

In summary, we have prepared homogeneous ceramics-polymer composites consisting of PZT particles as fillers and PVDF polymer as matrix, using a solution casting process. Composites film of PZT (Navy type-VI)-PVDF composition with PZT content of 0, 10, 20, 30, 40, and 50 volume % were fabricated and characterized. The flexibility of the composite could be retained when the ceramic loading was up to 50 vol.%. The relative permittivity ( $\epsilon_r$ ) increases and dielectric loss decreases with increase in the volume fraction of CCTO at all frequencies under study. Dielectric constant as high as 180 at 1 kHz was achieved. The SEM of the composites revealed the excellent distribution of PZT fillers in PVDF matrix.

### **Scope for Future Work:**

An application for polymer-composite film can be stretched to area of energy harvesting. So this work can be further extended to the studying of dielectric and piezoelectric properties after polling. Another characterization technique that can be used is to measure the temperature dependency of the dielectric permittivity and the loss factor. Moreover the ceramic films can be prepared through various other techniques such as by hot press or by tape casting method so as to compare the difference in the film uniformity, density of the composites prepared by different techniques.

## References:

1. Kwi-II Park et.al *Adv. Mater.* 2012, 24, 2999–3004
2. Ke Yu, et.al. *J. Appl. Phys.* 113, 034105 (2013);
3. T. R. Gururaja, A. Safari, R. E. Newnham and L. E. Cross, ‘Piezoelectric Ceramic–Polymer Composites for Transducer Applications’; *Electronic Ceramics*. Ed. by L. M. Levinson. Marcel Dekker, New York, pp. 92–128 (1988).
4. A.J. Moulson and J.M.Herbert, *Electroceramics-Materials-properties-applications* Chapman and Hall, London, (1990).
5. K.Uchino, *Piezoelectric Actuators and Ultrasonic Motors*, ed. H. Tuller, Kluwer Academic Publisher, Boston, (1997)
6. G. H. Heartling, *J. Am. Ceram. Soc.*, **82**, 797 (1999).
7. S.Elliot, *The Physics and Chemistry of Solids*, John Wiley and Sons, Chichester, p.560 (1998)
8. M. Zhu and P. Han, *Appl. Phys. Lett.*, **75**, 386 (1999).
9. Y.J. Park et al. / *European Polymer Journal* 41 (2005) 1002–1012 10.
10. [http://electrons.wdfiles.com/local--files/direction-electric-field-dependence-of-dielectric-constant/PVDF\\_Phase\\_Transition.jpg](http://electrons.wdfiles.com/local--files/direction-electric-field-dependence-of-dielectric-constant/PVDF_Phase_Transition.jpg) and [www.solvayplastics.com](http://www.solvayplastics.com)
11. A.Seema et.al. *Journal of Applied Polymer Science*, Vol. 106, 146–151 (2007)
12. A. Jain et.al. *Mechanics of Advanced Materials and Structures* (2014) **21**, 181–186
13. A.K. Zak et al. / *Ceramics International* 37 (2011) 1654 1653–1660
14. Y. Hu et al. *Ceramics International* 37 (2011) 1609–1613
15. P. Thomas et al. *Composites Science and Technology* 70 (2010) 539–545